Morphology and Thermal Properties of Poly(L-lactic acid)/ Organoclay Nanocomposites

Li-Huei Lin, Hsin-Jiant Liu, Neng-Kai Yu

Department of Chemical and Materials Engineering, Vanung University, 1 Van Nung Road, Chung-Li City, Taiwan, Republic of China

Received 26 September 2006; accepted 21 February 2007
DOI 10.1002/app.26477
Published online 19 June 2007 in Wiley InterScience (www.interscience.wiley.com).

ABSTRACT: A modified clay was used to prepare poly(L-lactic acid)/clay nanocomposite dispersions. X-ray diffraction and transmission electron microscopy experiments revealed that poly(L-lactic acid) was able to intercalate the clay galleries. IR spectra of the poly(L-lactic acid)/clay nanocomposites showed the presence of interactions between the exfoliated clay platelets and the poly(L-lactic acid). Thermogravimetric analysis and differential scanning calorimetry were performed to study the thermal behavior of the prepared composites. The properties of the poly(L-lactic acid)/clay nanocomposites were also examined as functions of the organoclay content. The exfoliated organoclay layers acted as nucleating agents, and as the organoclay content increased, the crystallization temperature increased. © 2007 Wiley Periodicals, Inc. J Appl Polym Sci 106: 260–266, 2007

Key words: composites; crystallization; differential scanning calorimetry (DSC); organoclay; thermogravimetric analysis (TGA)

INTRODUCTION

Poly(L-lactic acid) (PLLA) is a linear aliphatic thermoplastic polyester[1–3] produced from renewable resources; it has excellent properties comparable to those of many petroleum-based plastics and is readily biodegradable. PLLA is also one of the environmentally friendly polymers. It has very good mechanical properties, thermal plasticity, fabricability, and biocompatibility. Even when burned, it produces no nitrogen oxide gases and only one-third of the combustible heat generated by polyolefins and does not damage incinerators, and it thus provides significant energy savings. Therefore, PLLA is a promising polymer for various end-use applications, and currently there is increasing interest in using PLLA for disposable and degradable plastic articles. Such properties, allied with processability and good mechanical properties, make this polymer adequate for use in many biomedical applications such as wound closure, prosthetic implants, controlled-release systems, and three-dimensional scaffolds. The influence of the crystallinity on the glass-transition dynamics has been widely investigated in poly(ethylene terephthalate) (PET),[4–6] but this effect has been scarcely studied in poly(lactic acid)-based systems.[7] PLLA belongs to polyesters, such as PET, but the lamellar morphology is quite different; for example, PLLA exhibits higher long spacing than PET. Therefore, the study of this system may bring new insight to the general discussion of the effect of the crystalline phase on the segmental dynamics, a fundamental problem that is far from being fully understood.

The performance of PLLA can be enhanced by the incorporation of nanosized layered silicates. Recently, montmorillonite (MMT), a layered silicate with a lamellar shape, has attracted intensive research interest for the preparation of polymer/clay nanocomposites because its lamellar platelets display high in-plane strength, stiffness, and a high aspect ratio.[8] Typically, the chemical structure of MMT consists of two fused silica tetrahedral sheets sandwiching an edge-shared octahedral sheet of either magnesium or aluminum hydroxide. The Na^+ and Ca^{2+} residing in the interlayer galleries can be replaced by organic cations such as alkylammonium ions via a cation-exchange reaction to render the hydrophilic layered silicate organophilic. According to several recent works, the incorporation of nanolayers of mineral clay enhances the thermal stability,[9,10] mechanical strength,[11–15] and morphology[16–18] of PLLA.

In this study, we attempted to prepare PLLA/clay nanocomposites and then investigated the properties of the nanocomposites. The resulting materials were analyzed with X-ray diffraction to determine their morphological structure. Some thermogravimetric analysis (TGA) and differential scanning calorimetry (DSC) measurements were also performed to investigate the thermal and crystallization behavior of these

Correspondence to: H.-J. Liu (luiseliu@msa.vnu.edu.tw).

Journal of Applied Polymer Science, Vol. 106, 260–266 (2007)

compositions with respect to the nature and relative content of the organomodified clays.

EXPERIMENTAL

Materials

PLLA was purchased from Sigma (St. Louis, MO); its molecular weight was approximately 85,000–160,000 g/mol. Didodecyldimethylammonium bromide {DMAB; i.e., $[CH_3(CH_2)_{11}]_2(CH_3)_2NBr$} was purchased from Aldrich. All reagents and solvents were synthetic-grade and were used as received. The MMT clay (PK805) was supplied by Paikong Ceramic Materials Co. (Taoyuan, Taiwan).

Preparation of the organophilic clay

The organophilic clay was prepared by a cation exchange between the sodium cations of PK805 and quaternary alkyl ammonium cations of the intercalating agent.[19] During the cation-exchange reaction, MMT (5 g) was gradually added to an aqueous solution of DMAB or an intercalating agent at room temperature and stirred for 24 h. After the cation-exchange reaction, the obtained modified clay was washed repeatedly with deionized water until no AgCl precipitate was found during the titration of the filtrate with a 0.1*N* $AgNO_3$ solution. The wet modified clay was dried in a vacuum oven at 100°C for 12 h to remove water. The dried modified clay was ground to a powdery state and screened with a 325-mesh sieve.

Preparation of the PLLA/clay nanocomposite dispersions

Various amounts of organophilic clay (2, 3, 4, and 5 wt %) were individually mixed with 10 mL of tetrahydrofuran (THF). A typical procedure for the preparation of the PLLA/clay nanocomposite materials involved a 3 wt % clay loading. An appropriate mass of an organophilic clay (0.03 g) was introduced into 10 mL of THF with stirring for 12 h at room temperature. A PLLA powder (0.97 g) was added to the THF solution in another bottle, and then the polymer solution was stirred for 12 h at 60°C until it was homogeneous. The clay solution was added to the polymer solution with stirring for 12 h at 60°C. The PLLA/clay nanocomposite films were prepared by the casting of the solution onto glass plates. The films were dried in a vacuum oven for 4 h at 60°C.

Characterization

A Thermo model ARL X'TRA X-ray diffractometer (Ecublens, Switzerland) was used to examine the ordering in the clay and PLLA/clay nanocomposites. The X-ray beam was Ni-filtered Cu Kα radiation (wavelength = 0.154 nm) from a sealed tube operated at 45 kV and 40 mA. Data were obtained in the 2θ range of 0.5–30° at a scan rate of 1.5°/min. The transmission electron microscopy (TEM) observations were performed on a JEOL 2000E microscope (Tokyo, Japan) operating at 100 kV. A low-magnification image was taken at 10,000×. A high-magnification image was taken at 50,000×.

A PerkinElmer Spectrum One Fourier transform infrared (FTIR) spectrophotometer (Norwalk, CT) was used to identify the chemical structure of the PLLA/clay nanocomposites. The spectra were measured at a resolution of 4 cm^{-1}, and 32 scans were recorded per sample. The sample formed a thin film and was dried again in a vacuum oven at 60°C for 4 h. The surface morphological images of the composite films pretreated by Pt deposition were examined with scanning electron microscopy (SEM, model S-3000N, Hitachi, Ibaraki, Japan).

A PerkinElmer TGA-7 thermogravimetric analyzer (Norwalk, CT) was used to measure the weight losses of the PLLA/clay films in the temperature range of 40–500°C with a heating rate of 10°C/min and under a nitrogen flow of 20 mL/min. DSC was carried out with a PerkinElmer DSC-7 instrument (Norwalk, CT). An approximately 5-mg sample was placed in an aluminum pan. DSC scans were obtained from 25 to 190°C at a rate of 20°C/min, and then that temperature was maintained for 2 min. They were cooled to 25°C/min at a rate of 2°C/min.

RESULTS AND DISCUSSION

Morphology and structure of the PLLA/clay nanocomposites

The X-ray diffraction pattern was used to observe exfoliation in the clay nanolayers of PLLA with added clay. Figure 1 shows that the organophilic clay had X-ray diffraction peaks at $2\theta = 4^\circ$. The interlayer spacing calculated from the peak with the equation $2d \sin \theta - n\lambda$ (where d is the distance between the crystallographic planes, θ is half the angle of diffraction, n is an integer, and λ is the wavelength of the X-ray) was 2.2 nm accordingly. The characteristic diffraction peak at $2\theta = 4^\circ$, observed for the modified PK805 clay, disappeared, and this suggested that the clay layers were dispersed in PLLA.[20–22] The composite containing 5 wt % clay still could have completely exfoliated silicate platelets. DMAB enlarged the interlayer spacing of PK805 clay dramatically. Moreover, the hydrophilic clay became organophilic because of the presence of alkylammonium cations in the interlayer galleries.

To further study this, different amounts of the organophilic clay were mixed with PLLA, as shown

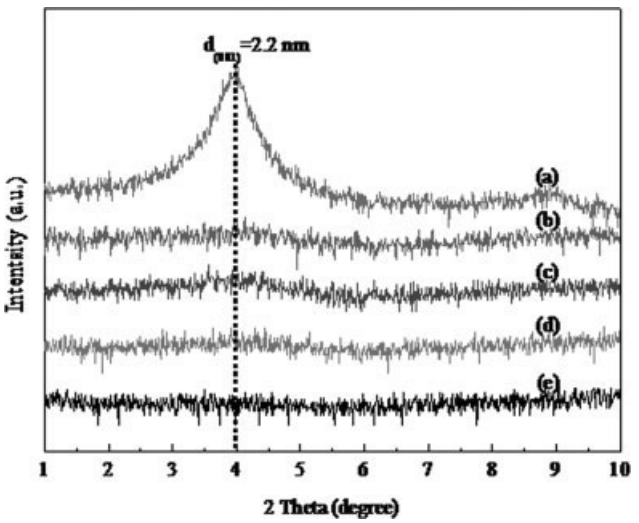

Figure 1 Various X-ray diffraction patterns through the addition of different amounts of organomodified PK805 to PLLA: (a) organomodified PK805 and (b) 2, (c) 3, (d) 4, and (e) 5 wt %.

in Figure 2. Each PLLA/clay nanocomposite exhibited a sharp diffraction halo at 2θ values of 16.5 and 19°, which corresponded to interlayer distances of 0.54 and 0.47 nm, respectively. The shapes of these peaks were not affected by the addition of the clay. These results imply that the clay layers were well dispersed in PLLA and that the PLLA structures did not change. The dispersion of the clay in PLLA was examined with a PLLA/clay composite containing 5 wt % clay through TEM. The micrograph is shown in Figure 3. The TEM image shows the clay to be well dispersed throughout the polymer. This conclusion is consistent with the X-ray results. By TEM, we observed that the nanolayers of the organophilic clay were well dispersed in the polymer chain, and this indicated that it may change the morphology of PLLA.

Figure 4 shows SEM images of the PLLA/clay nanocomposites containing various amounts of the clay. The domain size of the dispersed PLLA decreased with increasing clay content, and the films exhibited a nicely interconnected, closed-cell structure. Khatua et al.[23] attributed this decrease in the domain size to exfoliated clay platelets in the polymer blend effectively preventing the coalescence of the dispersed domains.

IR spectra of PLLA/clay films with clay contents of 0, 2, 3, 4, and 5 wt % are shown in Figure 5. The FTIR spectra display a characteristic band at 1044 cm^{-1} for PLLA; the intensity increases with the

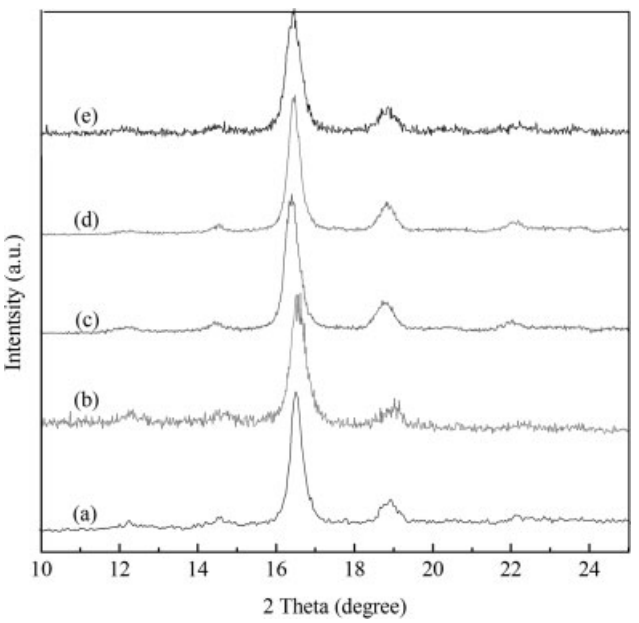

Figure 2 X-ray diffraction patterns of PLLA/clay nanocomposites with different clay contents: (a) 0, (b) 2, (c) 3, (d) 4, and (e) 5 wt %.

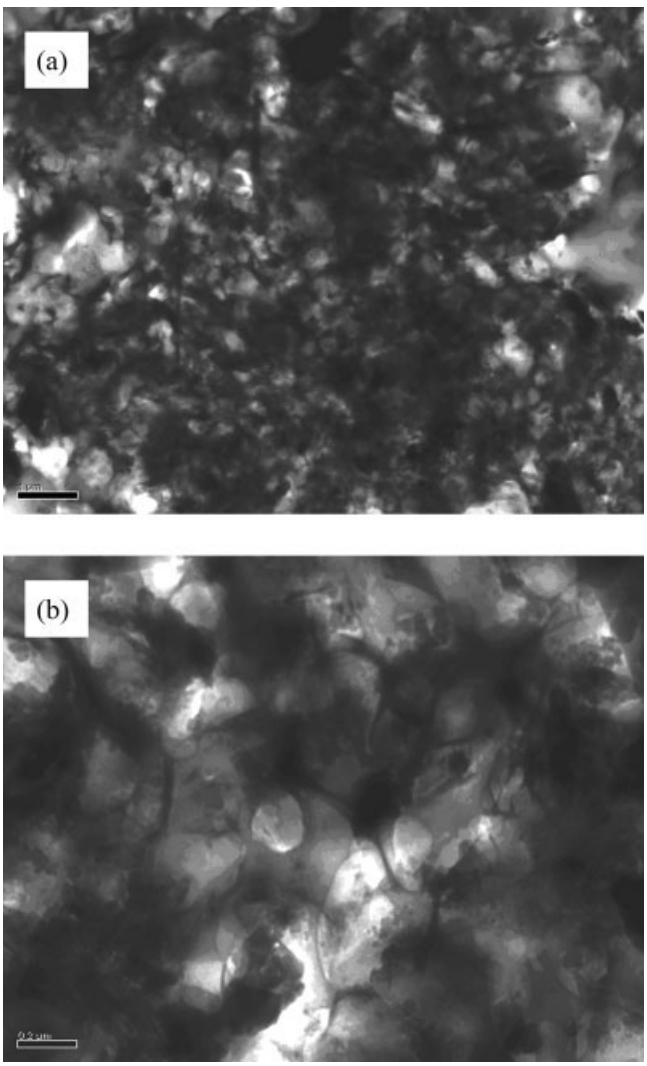

Figure 3 TEM images of a PLLA/clay nanocomposite with 5 wt % clay: (a) low magnification and (b) high magnification.

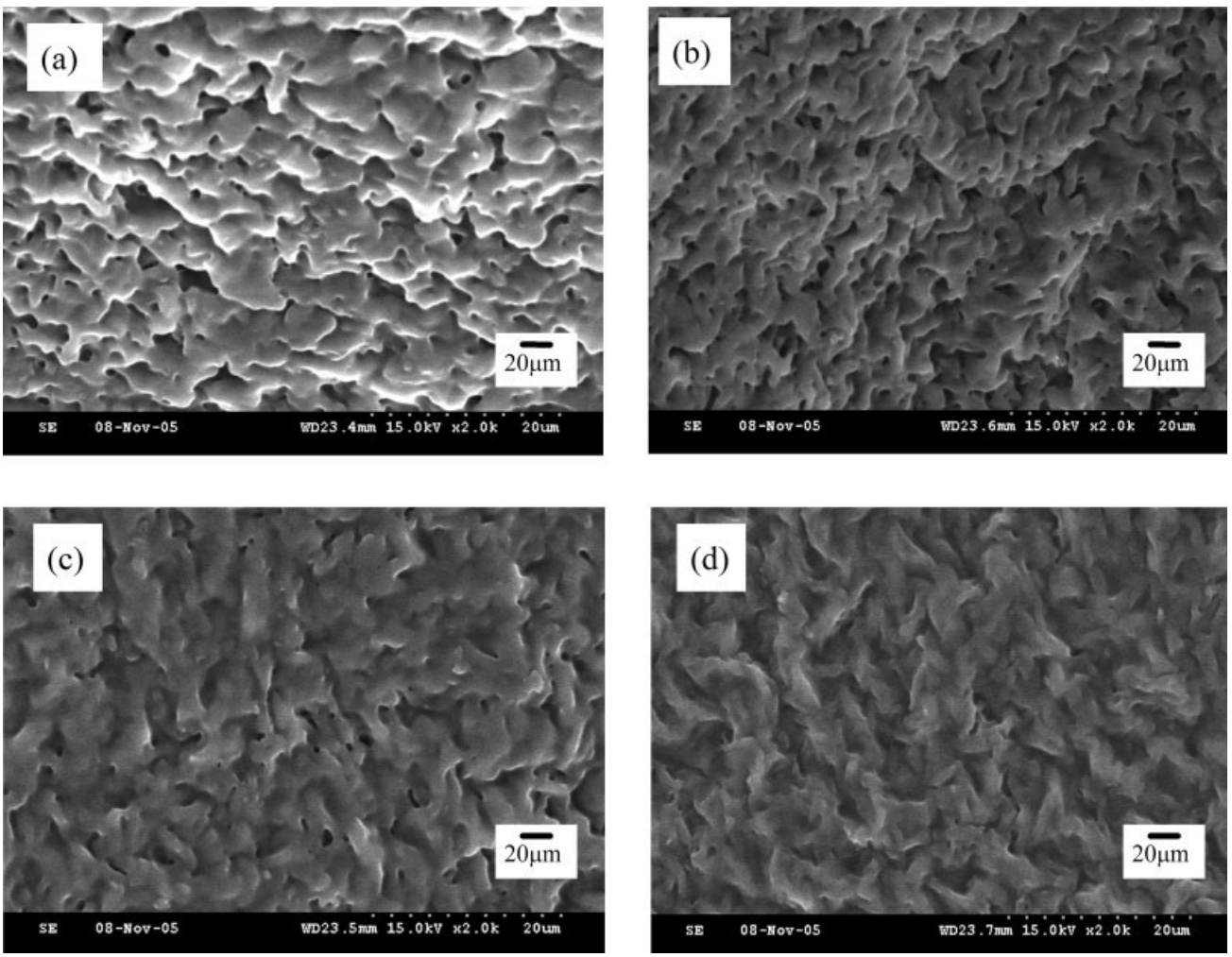

Figure 4 SEM micrographs of PLLA/clay nanocomposites with different organomodified PK805 contents: (a) 2, (b) 3, (c) 4, and (d) 5 wt % (2000×).

clay content. The band at 1757 cm^{-1} is assigned to the stretching vibration of C=O for PLLA. When the clay content increased, the absorption shifted to 1756 and 1749 cm^{-1}, and the carbonyl stretching was split into two peaks. Carbonyls usually undergo a significant change in the dipole moment for the corresponding vibrations, so the IR absorbance is intense for their vibrations. The carbonyl stretching region is normally a region with only one band in the absorbance of strong interactions such as hydrogen bonding. If there are multiple bands in the region, then because of the large dipoles of the C=O bond, there is the possibility of a dipole–dipole interaction being the relevant intermolecular force.[24]

Thermal properties of the PLLA/clay films

Because inorganic species have good thermal stability, it is generally believed that the introduction of inorganic components into organic materials can improve their thermal stability. This increase in the thermal stability can be attributed to the high thermal stability of clay and to the interaction between the clay particles and the polymer matrix.[25–27] Such enhanced thermal stability has already been reported for other composites with silicate layers based on matrices employing various types of organomodified MMTs.[28,29] Figure 6 shows the results of TGA measurements for PLLA/clay films with different clay contents. The degradation temperature of the PLLA/clay nanocomposites increased steadily from 250 to 300°C as the content of clay increased. Such behavior was explained by the relative extent of exfoliation. Indeed, at low clay contents in the PLLA/clay nanocomposites, exfoliation dominated, but the number of exfoliated silicate layers was not sufficient enough to promote any significant improvement in the thermal stability. Increasing the clay content led to more exfoliated individual platelets and increased the thermal stability of the composites. This enhancement of the thermal resistance with the presence of clay could be found when the PLLA/clay nanocom-

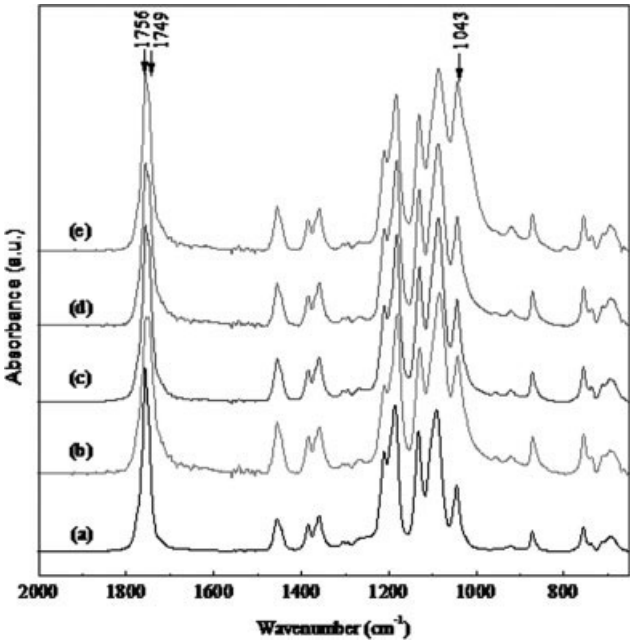

Figure 5 FTIR spectra of PLLA/clay nanocomposites with different organomodified PK805 contents: (a) 0, (b) 2, (c) 3, (d) 4, and (e) 5 wt %.

posite was heated above 350°C. The PLLA/clay nanocomposite containing more clay exhibited higher thermal resistance because of the high thermal insulation effect of the clay. The PLLA moiety was almost completely decomposed above 450°C. The PLLA/clay nanocomposite with a higher clay content exhibited a weightier residue at 500°C.

Figure 7 shows the DSC thermograms of PLLA/clay nanocomposites with different clay contents. Neat PLLA was melted at 173°C; the melting endothermic graph of PLLA shows one peak, but the PLLA/clay nanocomposites all show two melting

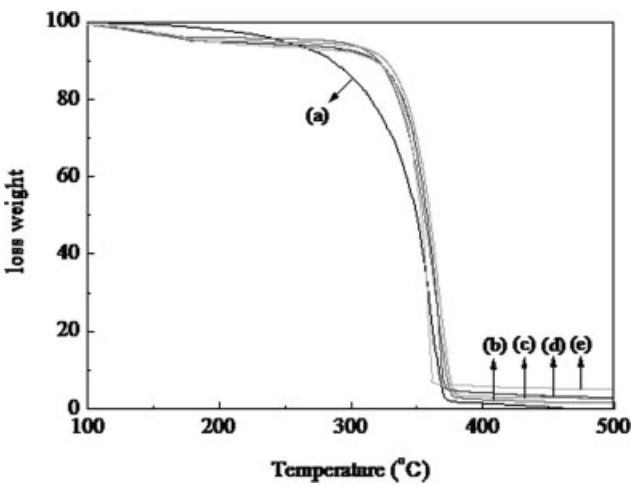

Figure 6 TGA curves of PLLA/clay nanocomposites with different organomodified PK805 contents: (a) 0, (b) 2, (c) 3, (d) 4, and (e) 5 wt %.

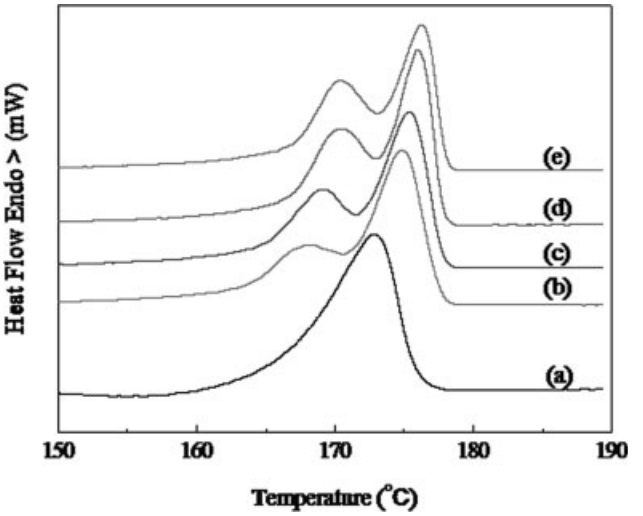

Figure 7 DSC thermograms of PLLA/clay nanocomposites with different organomodified PK805 contents from the heating scan (from 25 to 190°C at 2°C/min): (a) 0, (b) 2, (c) 3, (d) 4, and (e) 5 wt %.

peaks corresponding to the primary melting peak of PLLA. In addition, the melting temperature of the PLLA/clay nanocomposites increased gradually with increasing clay content. Figure 8 shows that at the cooling rate of 2°C/min, the pure PLLA crystallized slowly; therefore, the crystallization temperature was lower. However, with the addition of 2–5 wt % clay, crystallization peaks of PLLA were observed, with the peak temperature around 120°C, and the crystallization temperature increased with increasing organoclay contents. An endothermic peak for all samples in the temperature range of 120–130°C was found. The temperature corresponding to the endothermic peak for each sample was

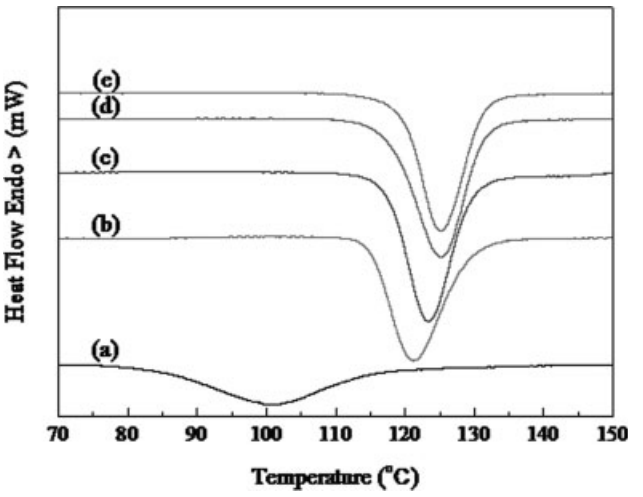

Figure 8 DSC thermograms of PLLA/clay nanocomposites with different organomodified PK805 contents from the cooling scan (from 190 to 25°C at 2°C/min): (a) 0, (b) 2, (c) 3, (d) 4, and (e) 5 wt %.

TABLE I
Crystallinity and Total Enthalpies of Fusion and Crystallization of PLLA/Clay Nanocomposites

Sample	T_c (°C)	ΔH_c (J/g)	T_{m1} (°C)	T_{m2} (°C)	ΔH_f (J/g)	χ_C (%)
Neat PLLA	100.9	−22.8	—	172.9	45.7	49.1
PLLA2PK805	121.3	−42.0	168.1	174.8	52.6	56.6
PLLA3PK805	123.3	−44.9	169.1	175.4	52.0	55.9
PLLA4PK805	125.1	−48.1	170.4	175.9	53.5	57.5
PLLA5PK805	125.1	−41.9	170.4	176.3	46.1	49.6

ΔH_c = enthalpy of crystallization; ΔH_f = enthalpy of fusion; χ_C = degree of crystallinity; T_c = temperature of crystallization peak; T_{m1} = temperature of melting peak 1; T_{m2} = temperature of melting peak 2.

considered to be the crystallization temperature of the PLLA/clay nanocomposite. For all samples, at the crystallization temperature, there was a steplike change due to enthalpy relaxation. These results show that clay exfoliated in the PLLA matrix resulted in an obvious increase in the crystallization rate compared with that of pure PLLA. This behavior can be explained by the assumption that exfoliated silicate layers act as efficient nucleating agents that enhance the crystallization rate of the polymer molecules.[30] Such behavior could be regarded as unique for polymer nanocomposites in which there exists a strong interaction between the organic surfactant covered on the surface of clay platelets and the functional groups on the main chain of the PLLA molecules.

The heat of fusion is shown as a function of the crystallization temperature for different nanocomposites and neat PLLA. Table I lists the calculated crystallinities.[31] The pure PLLA possessed a lower crystallinity than the PLLA/clay nanocomposites, and the crystallinity increased with increasing clay content. Moreover, the 5 wt % PLLA/clay nanocomposites had less crystallinity than the other samples. It could be concluded that with a higher extent of exfoliation, the 5 wt % PLLA/clay nanocomposites had the greatest effect in lowering the crystallinity of this composite system. At high organoclay contents, they became crystallization retardants, providing physical hindrance to restrict the molecular chain mobility of PLLA because of the increased interaction sites.

CONCLUSIONS

In this study, PLLA/clay nanocomposite dispersions were prepared with MMT clay and resulted in intercalation in THF as a cosolvent between PLLA and the organophilic clay. X-ray diffraction pointed out that quaternary alkyl ammonium salts could be used to increase the distances of the MMT clay interlayers to 2.2 nm, thereby allowing PLLA to enter the interlayer of the organophilic clay. TGA showed that increasing the clay content in the nanocomposite from 2 to 5 wt % affected the thermal resistance of the materials. The weight loss of the PLLA/clay nanocomposites increased with increasing clay content before 300°C. This was due to the presence of the organic alkylammonium compound used for clay modification. However, after the complete decomposition of the small organic molecules, the PLLA/clay nanocomposite containing more clay exhibited higher thermal resistance. The DSC results indicated that the melting temperature and degree of crystallinity of the PLLA/clay nanocomposites increased with increasing clay content and gradually shifted toward a higher temperature with increasing clay content. Therefore, the clay seemed to enhance the rate of crystallization of PLLA. It enhanced the crystallization temperature as the nanolayers of the organophilic clay dispersed into PLLA. The exfoliated organoclay platelets acted as nucleating agents at low contents by increasing the crystallization rate of PLLA.

References

1. Perego, G.; Cella, G. D.; Bastioli, C. J Appl Polym Sci 1996, 59, 37.
2. Tsuji, H.; Ikada, Y. J Appl Polym Sci 1998, 67, 405.
3. Martin, O.; Averous, L. Polymer 2001, 42, 6209.
4. Zhao, J.; Song, R.; Zhang, Z.; Linghu, X.; Zheng, Z.; Fan, Q. Macromolecules 2001, 34, 343.
5. Alves, N. M.; Mano, J. F.; Balaguer, E.; Meseguer Duenas, J. M.; Gomez Ribelles, J. L. Polymer 2002, 43, 4111.
6. Alvarez Sics, I.; Nogales, A.; Denchev, Z.; Funari, S. S.; Ezquerra, T. A. Polymer 2004, 45, 3953.
7. Manoa, J. F.; Gomez Ribelles, J. L.; Alvesa, N. M.; Salmeron Sanchez, M. Polymer 2005, 46, 8258.
8. Hwang, J. J.; Liu, H. J. Macromolecules 2002, 35, 7314.
9. Chen, G. X.; Yoon, J. S. Polym Degrad Stab 2005, 88, 206.
10. Paul, M. A.; Degee, P.; Henrist, C.; Rulmont, A.; Dubois, P. Polymer 2003, 44, 443.
11. Shibata, M. S. Y.; Orihara, M.; Miyoshi, M. J Appl Polym Sci 2006, 99, 2594.
12. Sinha, R.; Suprakas, M. P.; Okamoto, M.; Yamada, K.; Ueda, K. Macromolecules 2002, 35, 3104.
13. Ogata, N.; Jimenez, G.; Kawai, H.; Ogihara, T. J Polym Sci Part B: Polym Phys 1997, 35, 389.
14. Kubies, D.; Scudla, J.; Puffr, R.; Sikora, A.; Baldrian, J.; Kovarova, J.; Slouf, M.; Rypacek, F. Eur Polym J 2006, 42, 888.
15. Krikorian, V.; Pochan, D. J. Chem Mater 2003, 15, 4317.

16. Pluta, M. Polymer 2004, 45, 8239.
17. Chang, J. H.; An, Y. U.; Sur, G. S. J Polym Sci Part B: Polym Phys 2003, 41, 94.
18. Chen, C. X.; Yoon, J. S. J Polym Sci Part B: Polym Phys 2005, 43, 478.
19. Liu, H. J.; Hwang, J. J.; Chen-Yang, Y. W. J Polym Sci Part A: Polym Chem 2002, 40, 3873.
20. Morgan, A. B.; Gilman, J. W. J Appl Polym Sci 2003, 87, 1329.
21. Perrin-Sarazin, F.; Ton-That, M.-T.; Bureau, M. N.; Denault, J. Polymer 2005, 46, 11624.
22. Vermogen, A.; Masenelli-Varlot, K.; Seguela, R.; Duchet-Rumeau, J.; Boucard, S.; Prele, P. Macromolecules 2005, 38, 9661.
23. Khatua, B. B.; Kim, H. Y.; Kim, J. K. Macromolecules 2004, 37, 2454.
24. Kaoru, A.; Shaw, L. H. Macromolecules 2006, 39, 3337.
25. Zhu, Z. K.; Yang, Y.; Yin, J.; Wang, X.; Ke, Y.; Qi, Z. J Appl Polym Sci 1999, 3, 2063.
26. Bharadwaj, R. K.; Mehrabi, A. R.; Hamilton, C.; Trujillo, C.; Murga, M.; Fan, R.; Chavira, A.; Thompson, A. K. Polymer 2002, 43, 3699.
27. Jin-Hae, C.; Yeong, U. A.; Donghwan, C.; Emmanuel, P. G. Polymer 2003, 44, 3715.
28. Pramoda, K. P.; Liu, T.; Liu, Z.; He, C.; Sue, H. J. Polym Degrad Stab 2003, 81, 47.
29. Zong, R.; Hu, Y.; Wang, S.; Song, L. Polym Degrad Stab 2004, 83, 423.
30. Di, Y.; Iannace, S.; Maio, E. D.; Nicolais, L. J Polym Sci Part B: Polym Phys 2005, 43, 689.
31. Krikorian, V.; Pochan, D. J. Macromolecules 2004, 37, 6480.